AD-A161 622 WEATHER RADAR STUDIES(U) MASSACHUSETTS INST OF TECH 1/1
LEXINGTON LINCOLN LAB J E EVANS 31 MAR 85
DOT/FAA/PM-85-16 DT-FA01-80-Y-10546

UNCLASSIFIED F/G 4/2 NL

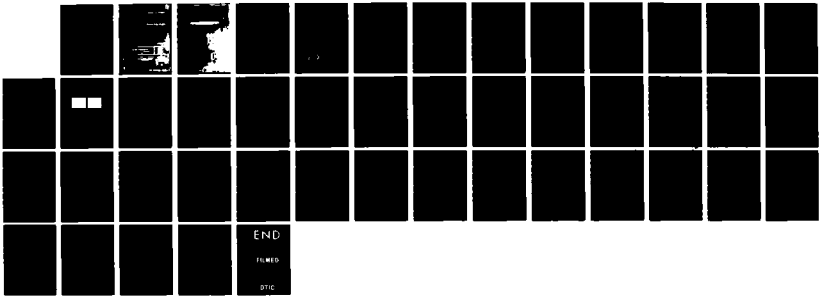

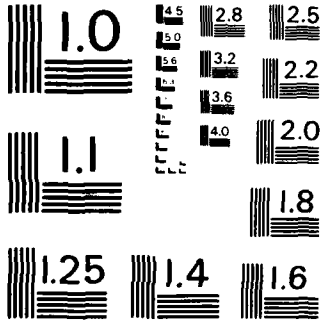

AD-A161 622

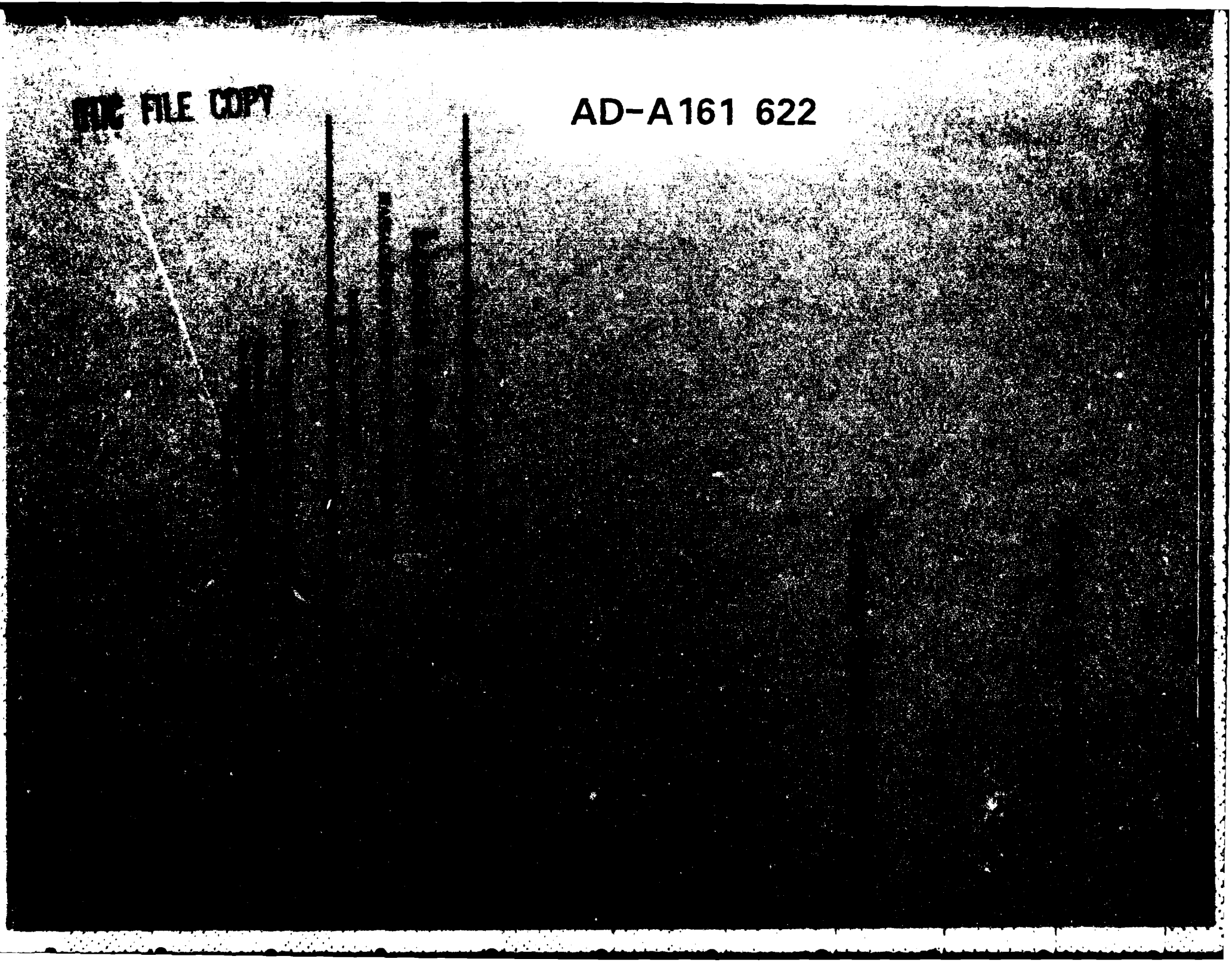

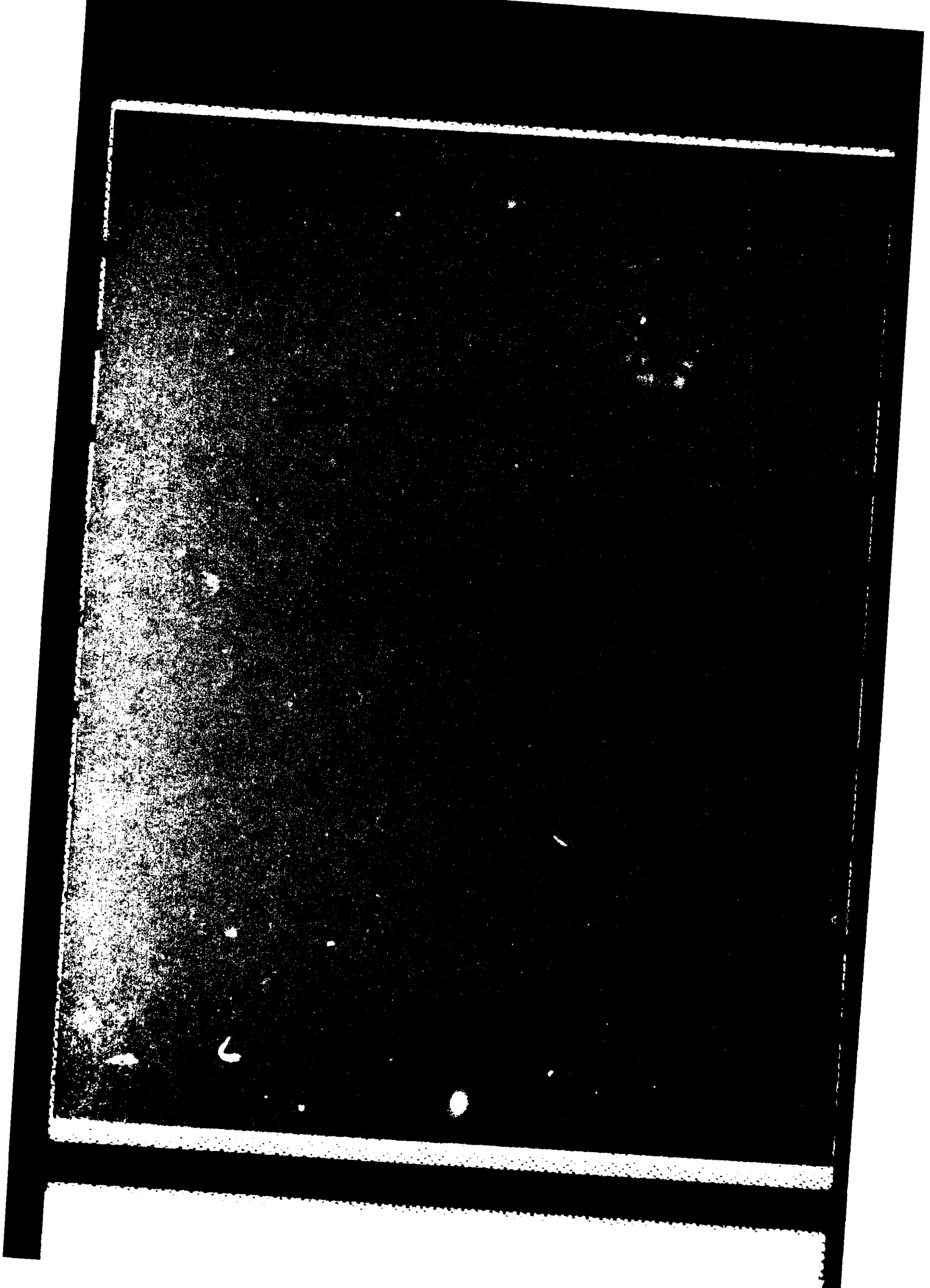

TECHNICAL REPORT DOCUMENTATION PAGE

1. Report No.	2. Government Accession No.	3. Recipient's Catalog No.
DOT/FAA-PM-85-16	AD-A161622	

4. Title and Subtitle	5. Report Date
Weather Radar Studies	31 March 1985
	6. Performing Organization Code

7. Author(s)	8. Performing Organization Report No.
James E. Evans	

9. Performing Organization Name and Address	10. Work Unit No. (TRAIS)
Massachusetts Institute of Technology Lincoln Laboratory P.O. Box 73 Lexington, MA 02173-0073	11. Contract or Grant No. DT-FA01-80-Y-10546
12. Sponsoring Agency Name and Address	13. Type of Report and Period Covered
Department of Transportation Federal Aviation Administration Systems Research and Development Service Washington, DC 20591	Quarterly Technical Summary 1 January — 31 March 1985 Issued 15 October 1985
	14. Sponsoring Agency Code

15. Supplementary Notes

The work reported in this document was performed at Lincoln Laboratory, a center for research operated by Massachusetts Institute of Technology, under Air Force Contract F19628-85-C-0002.

16. Abstract

FAA-funded Doppler weather radar activities during the period 1 January to 31 March 1985 are reported.

The test-bed Doppler weather radar system measurements in Olive Branch, Mississippi, commenced following the installation of an improved lightning protection system. Clutter suppression testing showed that the objective of 50-dB suppression was obtained in the field against appropriate fixed targets. Weather measurements were conducted on a number of cold front passages with attendant prefrontal lines of showers and thunderstorms.

The Lincoln mesonet was recalibrated at Lincoln in January and February and then installed at the site in late February. The mesonet was fully operational in March. The 1984 peak wind speed data from the mesonet and the Memphis International Airport LLWAS data were analyzed preliminarily to determine wind shear characteristics in the Memphis area.

Doppler weather radar data from the National Center for Atmospheric Research JAWS program and the National Severe Storms Laboratory are being analyzed to develop low-altitude wind shear detection algorithms. Analysis of the data collected in the 1983 Boston area coordinated aircraft-Doppler weather radar turbulence experiment commenced.

Work continued on the development of weather radar products for the Central Weather Processor with particular emphasis on the correlation tracking and extrapolated weather map algorithms.

17. Key Words		18. Distribution Statement
weather radar low-altitude wind shear NEXRAD	Central Weather Processor aviation weather products turbulence	Document is available to the public through the National Technical Information Service, Springfield, VA 22161.

19. Security Classif. (of this report)	20. Security Classif. (of this page)	21. No. of Pages	22. Price
Unclassified	Unclassified	48	

FORM DOT F 1700.7 (8-69)

ABSTRACT

FAA-funded Doppler weather radar activities during the period 1 January to 31 March 1985 are reported.

The test-bed Doppler weather radar system measurements in Olive Branch, Mississippi, commenced following the installation of an improved lightning protection system. Clutter suppression testing showed that the objective of 50-dB suppression was obtained in the field against appropriate fixed targets. Weather measurements were conducted on a number of cold front passages with attendant prefrontal lines of showers and thunderstorms.

The Lincoln mesonet was recalibrated at Lincoln in January and February and then installed at the site in late February. The mesonet was fully operational in March. The 1984 peak wind speed data from the mesonet and the Memphis International Airport LLWAS data were analyzed preliminarily to determine wind shear characteristics in the Memphis area.

Doppler weather radar data from the National Center for Atmospheric Research JAWS program and the National Severe Storms Laboratory are being analyzed to develop low-altitude wind shear detection algorithms. Analysis of the data collected in the 1983 Boston area coordinated aircraft-Doppler weather radar turbulence experiment commenced.

Work continued on the development of weather radar products for the Central Weather Processor with particular emphasis on the correlation tracking and extrapolated weather map algorithms.

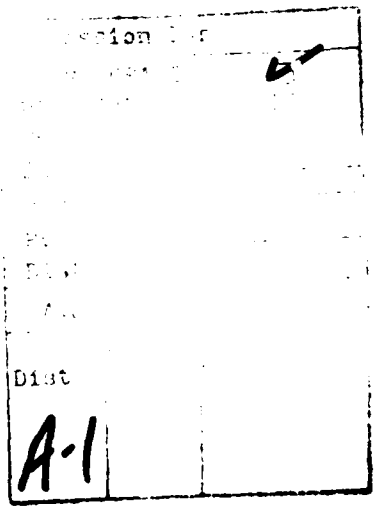

TABLE OF CONTENTS

LIST OF ILLUSTRATIONS

LIST OF TABLES

WEATHER RADAR STUDIES

I. INTRODUCTION

The principal areas of emphasis for the weather radar program over the period January-March 1985 have been:

(a) Development of a transportable Doppler weather radar test-bed to be utilized in a series of experimental programs during 1985-87.

(b) Reduction of data from the coordinated Doppler weather radar-aircraft experiments in the Boston, Massachusetts, area during the summer of 1983 and other Doppler weather radar measurement programs in the Denver and Oklahoma areas.

(c) Commencement of the first set of transportable test-bed experiments in the Memphis, Tennessee, area.

(d) Development of detailed specifications for certain Central Weather Processor (CWP) products to be generated by the NEXRAD system.

Progress in each of these above areas is described in the sections that follow.

II. TEST-BED DEVELOPMENT

The principal objectives for the transportable test-bed have been to develop a NEXRAD-like Doppler radar which can be used for:

(a) Resolving the principal uncertainties in algorithms for detection and display of en route and terminal hazardous weather regions.

(b) Obtaining feedback from operationally oriented users on the utility of strawman end products for improving safety and efficiency of airspace utilization.

(c) Investigating Doppler weather radar -- CWP interface issues.

(d) Providing a data base for FAA specification of NEXRAD, terminal weather radar, and NEXRAD CWP interfaces.

During the 1985-86 experiments, the transportable test-bed radar (hereafter referred to as FL-2) will be used in the following modes:

(a) As a terminal Doppler weather radar to detect low-altitude wind shear (LAWS) and other hazards both:

  (1) 'On-airport' using 360° PPI scans with principal focus on glide slope headwind tailwind shear, and

  (2) 'Off-airport' using sector PPI scans with occasional RHI scans to focus on microburst downburst detection in midair stage.

(b) As a NEXRAD 'network' sensor with a 5-min volume scan and principal focus on products of particular interest to the FAA such as turbulence, layered reflectivity, and LAWS.

(c) For 'scientific' data acquisition (as in the JAWS Project and NSSL Spring Programs characterized by scientist-controlled scan patterns based on real-time three-moment displays.

Figure II-1 shows a block diagram of the FL-2 test-bed.

The FL-2 activity during the quarter focused on completing the integration testing, installation of an improved lightning protection system, and commencement of measurements. Useful measurements commenced in February and full meteorological measurements in March. The development focus has turned to accomplishing refinements to the initial operating capability.

A. RADOME

The radome continued to operate satisfactorily throughout the period. No deflations occurred and the backup diesel generator did not have to be utilized.

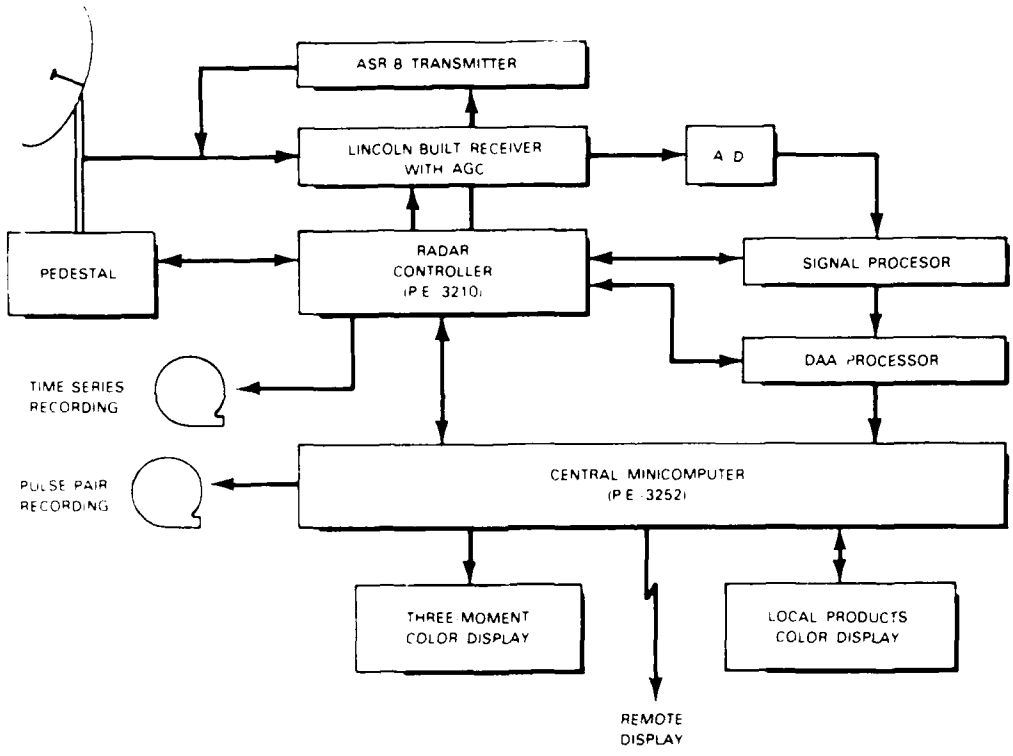

Figure II-1 FL-2 test-bed block diagram.

B. ANTENNA

Sun measurements with the antenna yielded a 1.2-dB one-way waveguide and feed-horn loss. This loss is viewed as reasonable for the system.

C. ANTENNA MOUNT

An oil leak in the elevation gear box caused oil to drip onto one of the drive clutches resulting in slippage. The leak was repaired and the clutch disassembled, cleaned, and rebuilt. A problem of grease breakdown was discovered and a different lubricant now has been installed. Routine monthly checks turned up loose bolts (cured by use of elastic stop-nuts), loose turnbuckles on guy wires (cured by readjusting and safety wiring), and a deteriorated O-ring in the oil pump (replaced).

Study of the drive servo system continues in an effort to characterize its behavior and specify a model for use in generation of antenna control programs. A decision was made to digitize and make available to the 3210 computer the output from the pedestal drive tachometers. These signals will permit a direct reading of rotation velocities.

Characterization of the antenna mount servo performance analysis continued. Table II-1 compares the currently achieved antenna capability with that at the FAA Technical Center prior to gearing and servo changes. The pedestal peak velocities and accelerations meet the overall requirements. However, the rate servo loop bandwidths are too small. This results in overshoots in coming to a stop in some situations and hence increases the overall time to perform the strawman scan sequences described in the previous quarterly progress report. The rate servo bandwidths will be increased in the next quarter to permit operation more nearly approximating the acceleration limits.

TABLE II-1

Pedestal Performance at FAATC vs Memphis

Feature	FAA Technical Center	Memphis
Azimuth Speed (deg/s)	15	30
Commanded	6, 12	2-30
Observed	6, 12	2-30
Elevation Speed (deg/s)	15	15
Commanded	—	2-15
Observed	—	2-15
Azimuth Acceleration (deg/s^2)	15	15
Expected	10	15
Observed (Computer)	—	10-14+ at 0.90 degrees elevation
Observed (Manual)	—	18-22
Elevation Acceleration (deg/s^2)	15	15
Expected	—	15
Observed (Computer)	—	14.5+
Observed (Manual)	—	14.6-15.5
Operating Modes:		
PPI Sector Scan	Yes	Yes
Volume Scan	Manual	Yes
RHI Sector Scan	No	Yes
Volume Scan	No	Yes

D. TRANSMITTER/RECEIVER

The cause of three spurious components in the transmitter spectrum was discovered. The 120-Hz component was due to ripple in the modulator core-bias power supply and was reduced to the general noise level by the addition of a filter capacitor. The components at 60 and 180 Hz are due to the ac klystron filament supply. A study is under way to reach a cost-effective cure by shielding or use of a dc power supply.

The receiver and waveguide system was calibrated using received solar radiation. An internal test-target generator was installed and calibrated. This equipment can be controlled digitally from the Perkin-Elmer 3210 computer and will be used to calibrate and monitor performance of the complete receiving system exclusive of waveguide and antenna.

E. SIGNAL PROCESSOR

The test-bed signal processor is a hard-wired computation unit, designed to perform the front-end processing of weather radar data. This processing consists of three basic parts: AGC compensation, clutter filtering, and autocorrelation processing as shown in Figure II-2.

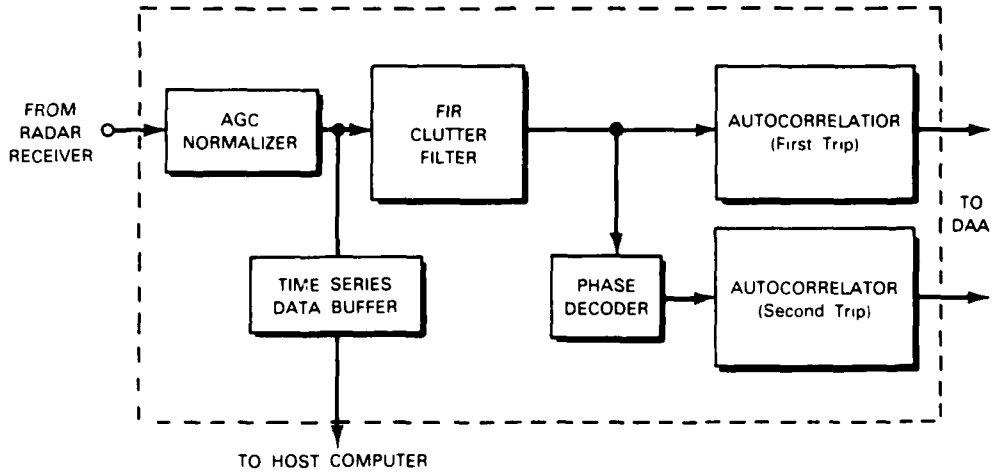

Figure II-2. Signal processor architecture.

The signal processor (SP) filters were debugged and integrated with the autocorrelators, thus providing full capacity for first-trip processing. Problems were found with control lines between the autocorrelators and the data acquisition and analysis (DAA) that were caused by crosstalk. This was corrected by adding balanced line drivers and receivers and additional cables. Also, twisted pair wires were added to the SP backplane to correct noise induced timing errors.

Currently, SP testing is accomplished using a radar simulator in place of the A/D converters and diagnostic programs that run in the DAA and the P.E.-3210. The simulator is limited in its ability to test the SP thoroughly because of small memory size and manual control. The current test sequences are sinusoids and 'white noise'.

A new simulator is being designed that will become an integral part of the SP and will provide extensive test features under computer control. The simulator will have sufficient memory capacity to provide realistic simulation of the radar signal including gate-to-gate variations. A second SP for use at Lincoln is under construction and will be available for checkout in the next quarter. This SP will enable us to debug and integrate SP features at Lincoln rather than the test site as well as to furnish more realistic inputs to the DAA processor at the Laboratory.

Figure II-3 shows the clutter rejection capability of the signal processor against clutter from the moving target simulator (MTS) tower. The left hand figure is the spectrum of return from the MTS and the tower. The MTS signal is seen to have a return power some 35-dB below the tower return. The right hand figure shows the spectrum of the signals at the output of the clutter filter section where the MTS signal is now some 17 dB above the residue clutter from the tower. The clutter suppression in this case is thus 17 - (-35 dB) = 52 dB which exceeds the NEXRAD Technical Requirement by 2 dB.

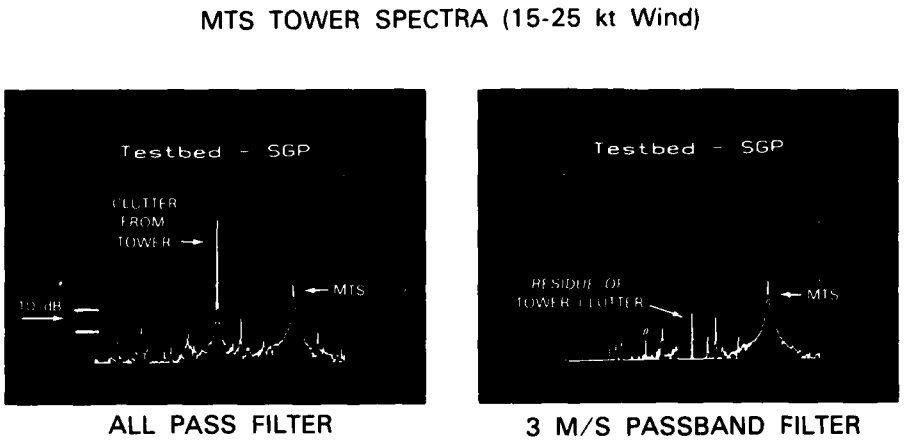

150544-N-01

Figure II-3. Signal processor clutter filter performance on moving target simulator (MTS) signal from tower.

F. DATA ACQUISITION AND ANALYSIS PROCESSOR

A total of fourteen processing element boards will be built. At present, nine boards have been built, seven have undergone modification and are working. The modifications increase a board's processing capability and speed.

A second DAA, to reside at Lincoln, is under construction. This second DAA will enable personnel to debug boards and develop software simultaneously, therefore increasing throughput.

The Input Multiplexor board, whose purpose is to read from the time code generator, the antenna, and the single gate procesor (SGP) data port, has been installed and tested at the radar site. A copy of this board, for the development system at Lincoln, is under construction.

A general purpose mechanism for sending messages between processing modules is fully operational. This mechanism is the primary means of communication between tasks. This communication mechanism will enable us to run complete simulations on software modules and therefore aid in the reduction of installation time of DAA software into the FL-2.

Work continues on the autocorrelation lags-to-factors conversion, resampling of the data from the (r, θ) measurement grid to a Cartesian grid, and implementation of a clutter mapping capability.

G. RADAR/ANTENNA CONTROLLER

No significant enhancement to the radar/signal processor/DAA control capabilities occurred during the period.

An offline clutter filter test program was developed for testing of the signal processor (SP) by downloading simulated time series samples into a RAM for input to the SP in place of A/D samples. This test was used to verify proper operation of the filters.

Assessment and optimization of the antenna control system software proceeded this quarter in conjunction with the control systems engineers from Division 7. Tests of the antenna with the strawman PPI sector scan and RHI scan sequences showed scan durations that were approximately 25 percent slower than desired. Subsequent modification of the position servo loop enabled us to reduce the scan times to move from one fixed angle position to another to nearly the acceleration limited time for position steps $<10°$. We now are focusing on developing mount data recording and offline analysis software to permit optimization of the mount scan algorithms that do not meet the design goals.

H. MAIN MINICOMPUTER

An initial operating capability for data recording and display was achieved on the Perkin-Elmer 3252 computer in January and the system successfully used for measurements in February and March. The current display and recording capability is not satisfactory due to problems in handling the full volume of lags data from the DAA. This has resulted in having the antenna scan slower and radiate at a PRF that is lower than desired so that all the range gates can be recorded. This problem will be resolved by the next version of the DAA software, which will perform the bulk of the front-end processing, hence unloading the P.E.-3252.

The departure of staff and contractor personnel responsible for the initial 3252 programs has further slowed progress in refining the 3252 software. Two contract programmers were hired at the end of the quarter and are becoming familiar with the system. The high priority items for the coming quarter are:

(1) achieving real time display of designated aircraft positions as an overlay to weather data on the 3-moment displays so that coordinated aircraft/radar experiments can commence in late May,

(2) preparing a real-time system to accept next-generation DAA outputs, and

(3) improving the user interface for scan sequence inputting.

It has been noticed that the Perkin-Elmer computers perform erratically when the antenna radiates energy in their direction. Lincoln Laboratory personnel have been working with Perkin-Elmer in an attempt to isolate the equipment that picks up the radiation. Most tests performed so far have led to negative results, with one exception. There is strong evidence that the read amplifier modules for magnetic tape drives are affected, and a spare module is being procured for

testing various modifications. Other offending areas in the computers have not been isolated. The possibility of screening the entire computing system was considered, but the logistics of such a task have relegated it to a last resort. The geometry of the Olive Branch site is such that data collection is affected only marginally because the antenna seldom is pointed directly at the computers. However, a solution must be implemented, and a major effort is continuing.

I. FL-2 ENHANCEMENTS

Considerable effort was expended during the quarter in obtaining suitable workstations to act as product displays in ATC facilities over the next few years. A request for information (RFI) was issued to major workstation and display vendors for a system which could:

(1) receive compressed weather images, aircraft locations, etc., over a phone line at 9600 b s using the High Level Data Communications (HDLC) (a subset of X.25) transfer protocol in a synchronous communication mode,

(2) store the images on a local disk, and

(3) display selected images on a high-resolution color display (e.g., nominally 900 × 900 pixels with 256 color options) with hardware zoom.

The workstation will enable one to display a variety of candidate CWP and terminal weather radar products as well as a simplified ATC display (e.g., aircraft positions with beacon codes and altitudes plus standard ATC overlays) for evaluation of weather product utility and validity. The local workstation will permit site personnel to monitor the remote display products as well as acting as a local product display for experiment control.

The analysis of vendor responses has been completed. We anticipate placing an order for and receiving three Apollo workstations in the next quarter.

III. SITE OPERATIONS AND SUPPORTING SENSORS

A. MEMPHIS SITE MODIFICATIONS

1. Lincoln Radar Site

An extensive modification to the prime power and grounding system was accomplished to improve power reliability during storms and to provide improved lightning protection to the site. A large (350 kW) engine generator was acquired and brought on line to be used whenever there are storms in the area and loss of commercial power is likely. Figure III-1 shows the current power distribution system at the site.

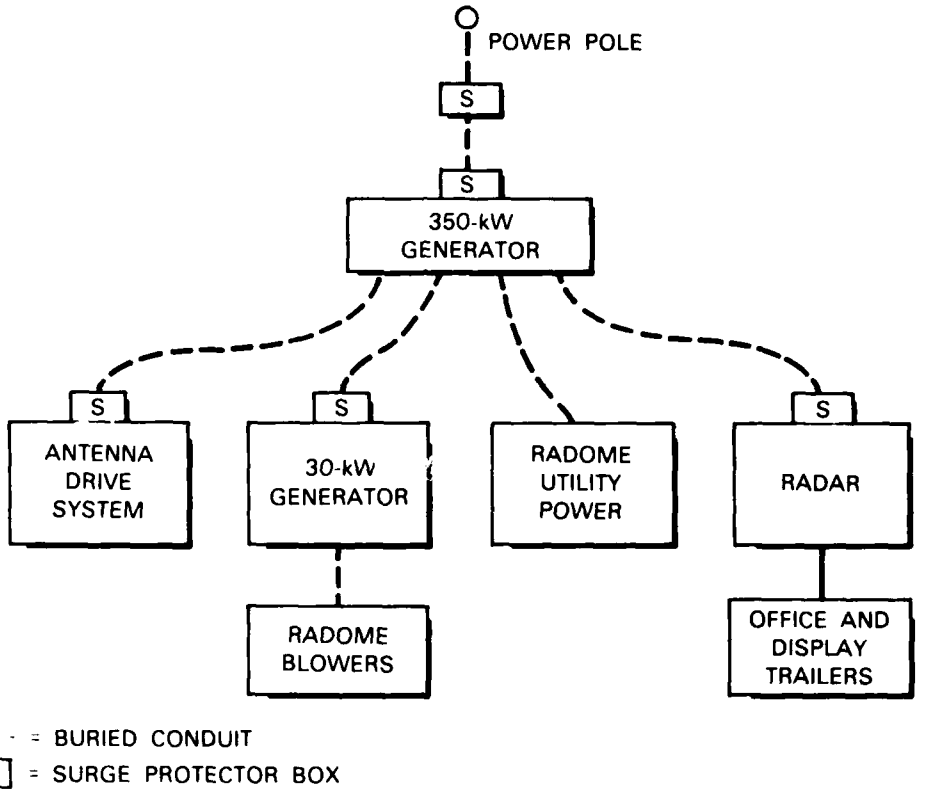

148840-N

Figure III-1. Site power distribution.

Personnel from the FAA Power Systems Branch visited the site to make many improvements in chassis, power, and signal ground methods. As a result, ground-loop noise should be minimized and personnel safety should be assured. The on-site lightning protection hardware was evaluated with several suggestions made and implemented. It now is felt that the site is as lightning-tolerant as reasonably can be expected. Additionally, voltage and frequency

monitors were installed that cause an alarm to be sounded if prime power quality strays outside preset limits.

The parking lot area top layer of mud was removed and replaced by crushed stone to alleviate the problem of supplier and visitor vehicles being stuck during rain periods.

2. University of North Dakota (UND) Site

The UND site preparation including installation of an engine generator was completed during the quarter. The UND mount, antenna, and radome were installed on the Lincoln tower in late March and the radar declared operational on 1 April.

3. Mesonet Sites

No mesonet site changes occured during the quarter. Favorable weather permitted installation of all sensors and data collection platforms in February.

B. HUNTSVILLE SITE PLANNING

Plans were solidified this quarter to move the test-bed and mesonet to Huntsville. During the next quarter, we hope to determine exact locations for the Lincoln and UND radars, approximate locations for the mesonet stations, and to commence discussions with the landowners.

C. MEMPHIS SITE OPERATIONS

1. FL-2 Measurements

The FL-2 radar became operational early in the quarter and was being fully utilized for meteorological operations by early March. The initial taped data collected in February was primarily for testing purposes.

One series of measurements being made on a fairly routine basis is a sequence of scans designed to measure the ground clutter from the radar. The same scans are run weekly to evaluate, among other things, the changing effects of leaves coming out on the trees in the vicinity during the transition from winter to spring and into summer. This sequence will continue to be run through the operational season and should provide some interesting data on the effects of vegetation on ground clutter variability.

The first meteorological data were collected on 4 March 1985. Through the end of the quarter, a total of 44 data tapes had been collected (37 of which were of meteorological situations) as summarized in Table III-1. The dominant weather pattern sampled during this early period was the passage of cold fronts with their attendant prefrontal lines of showers and thundershowers. As of the end of the quarter, no significant wind shear events were detected during the real-time observation of the data being collected; however, a thorough reanalysis of these same data possibly might reveal some weak events that went undetected during operations.

TABLE III-1

FL-2 Radar Measurements at Olive Branch, Mississippi, During First Quarter of 1985

Date	Tapes Recorded	Weather Conditions
8 Feb.	1	fair (clutter tape)
20 Feb.	1	fair (display test tape)
21 Feb.	1	fair (noise test tape)
4 Mar.	5	thin echo line with 40-50 dBz echoes, no thunder tops to 15 kft., 0.43 inches rain
11 Mar.	1	fair, windy (clutter tape)
12 Mar.	1	weak rain to northwest near Missouri
18 Mar.	1	fair (clutter tape)
25 Mar.	1	fair (clutter tape)
27 Mar.	9	thunderstorms with 0.47 in rain
30 Mar.	21	thunderstorms with peak reflectivities to 65 dBz, but not windy — measurements from 0800 to 2300 CST

2. Mesonet Operations

Lincoln has been operating a 30-station mesonet in the Memphis area since early 1984. The individual stations (obtained originally from the Bureau of Reclamation and substantially upgraded by Lincoln) record a 1-min average of temperature, pressure, humidity, winds, and precipitation. The results from the past half hour are telemetered to a GOES satellite every 30 minutes and then transmitted down to the Synergetics Corporation ground station. Lincoln receives a data tape from Synergetics weekly with the data for the various stations.

The mesonet sensors were recalibrated and upgraded in January. Specific changes were as follows:

(1) barometers — additional lengths of heater wire were added and the Data Collection Platform (DCP) software upgraded after the barometers were calibrated in the Lincoln Space Laboratory,

(2) wind speed and direction sensors — replacement of defective parts (e.g., screws and shaft assemblies),

(3) Vane aspirators — replacement of bad bearings prior to cleaning and painting,

(4) temperature/relative humidity probes — installation of new filter-caps after calibration by Vaisala Corporation and

(5) voltage regulators — upgrade to 9-volt operation to improve measurement sensitivity.

All mesonet equipment was shipped down to Memphis on 8 February and it arrived on the fourteenth. Initial deployment of sensors began on the fifteenth. Each site was visited twice: the first time to deploy the calibrated sensors and the second time to turn on the rain gauges, paint the outside of the white armored boxes, and to install the newest revision of the software. The software setup had to be changed to eliminate the loss of resolution in wind direction angle around 180° and 360° resulting from the use of the cosine only. The new program transmits sine instead of cosine from 315°-45° and from 135°-225°.

All 30 stations with all of their sensors were completely operational by the end of the month. This achievement surpassed a goal set in August 1984 of having the network completely operational by 4 March 1985. All of those responsible for this work, beginning with the removal of the sensors last December, through the calibration work in January and the testing and deployment in February, have done an excellent job and are to be commended. Thunderstorm winds (the first this season) of about 75 mi/h were recorded in the network during the last week in February (all stations in the vicinity were operating), and the network was fully operational for the 4 March frontal storm (58 mi/h gusts) for which radar data was recorded as well.

A program was written that will plot mesonet data in the format in which it is received over the phone from Synergetics and make it much easier for FL-2 personnel to identify sensor and/or data problems on a daily basis.

The single problem with the mesonet data is that the pressures reported by the mesonet stations initially were averaging about 19 mb too high. Individual stations were observed to give averages larger and smaller than this overall average error. Further, the pressures from individual stations vary from day to day, depending upon the absolute pressure and the ambient temperature. We have determined adjustments to the pressure calibration constants to account for the large offset, but will have to correct for the smaller departures on a case study basis.

In the course of investigating this problem, it became evident that some of the calibration constants for the slope of the calibration curves at individual stations are somewhat in error. We have not attempted to change the slopes but have changed the intercept values to give better pressures. The effects of temperature on the pressures reported by individual stations have not been and likely cannot be addressed easily during this field season. However, temperature either must be accounted for in the calibration equation directly or must be better controlled in order to give more accurate and reliable pressure measurements for next season.

3. Low Level Wind Shear Alert System (LLWAS) Recording System Operations

Lincoln has been recording the Memphis International Airport Low Level Wind Shear Alert System (LLWAS) data continuously since the summer of 1984 on a Lincoln-developed recording system. Weekly, the site personnel go to the Memphis tower to change data tapes. The LLWAS recording system worked reliably throughout the quarter.

4. UND Radar Measurements

No UND weather radar measurements were conducted during the quarter.

5. Aircraft Support

The UND plane was scheduled to arrive in Memphis for one month of measurements in mid-May.

6. Additional Weather Data

The recording system to store RRWDS data on magnetic tape for later playback became operational. The recorder operates in parallel with the real-time display and can store about 24 hours of data on a single reel of tape. The RRWDS data tapes are being saved for all days on which the Lincoln radar makes weather measurements. Data also are being retained from the Harris Laserfax recorder (for satellite images) and the Alden Difax recorder (for weather charts).

7. Additional Clutter Data

No clutter data from sites other than Memphis were collected this quarter.

IV. EXPERIMENTAL DATA REDUCTION AND ALGORITHM DEVELOPMENT

A. PERKIN-ELMER COMPUTER SYSTEMS

During this quarter, project participants enjoyed access to two complete Perkin-Elmer (P.E.-3242) computer systems. The machines access similar, though not identical, peripheral devices, and operate under revision 7.2 of the OS/32 operating system. By the end of the quarter, both machines contained eight megabytes of main memory. The systems were configured so that programs developed on one machine could be run on the other with no changes. Contrary to our experience in the previous quarter, both machines have performed fairly reliably, with some minor problems with peripheral devices.

The user load has grown steadily over the quarter. Most daytime software development takes place on one machine, with real-time P.E.-3252 and DAA software development being performed on the other. During the third shift, both machines are available for batch processing and disk backup procedures. Typically, there are 6 to 8 users per machine during the day at a time with a total of approximately 28 users.

The Perkin-Elmer computers provide a satisfactory data processing environment although the processing backlog grew significantly during the quarter. The software development environment provided by the machines also is satisfactory, but less so. This situation is due primarily to system bugs and idiosyncracies, a poor editor, and antiquated (where available) software development tools. Perkin-Elmer is making the UNIX operating system available to customers, but does not currently support the optimizing compiler under that system; that compiler is very important in making effective use of the computers.

While the systems have been performing well recently, past problems with Perkin-Elmer maintenance procedures have noticeably affected user morale and confidence. It is hoped that Perkin-Elmer can continue to show improvement in their handling of our hardware and software problems.

B. RADAR DATA ANALYSIS SOFTWARE DEVELOPMENT

Figure IV-1 summarizes the overall data analysis software structure. The programs that translate Universal format radar data into Common Format Tape data (CFT) have been consolidated into one user-interactive program. There is now the capability to translate into CFT data from MIT experiments in 1983, NSSL 'universal format' data (including JDOP), and universal format data from the JAWS experiment. Still to be written are translators to handle UND 'raw' radar data and an old MIT radar format.

The capability to derive new CFT (r, θ) fields from existing CFT data now is well developed. Programs are available to derive various shear products.

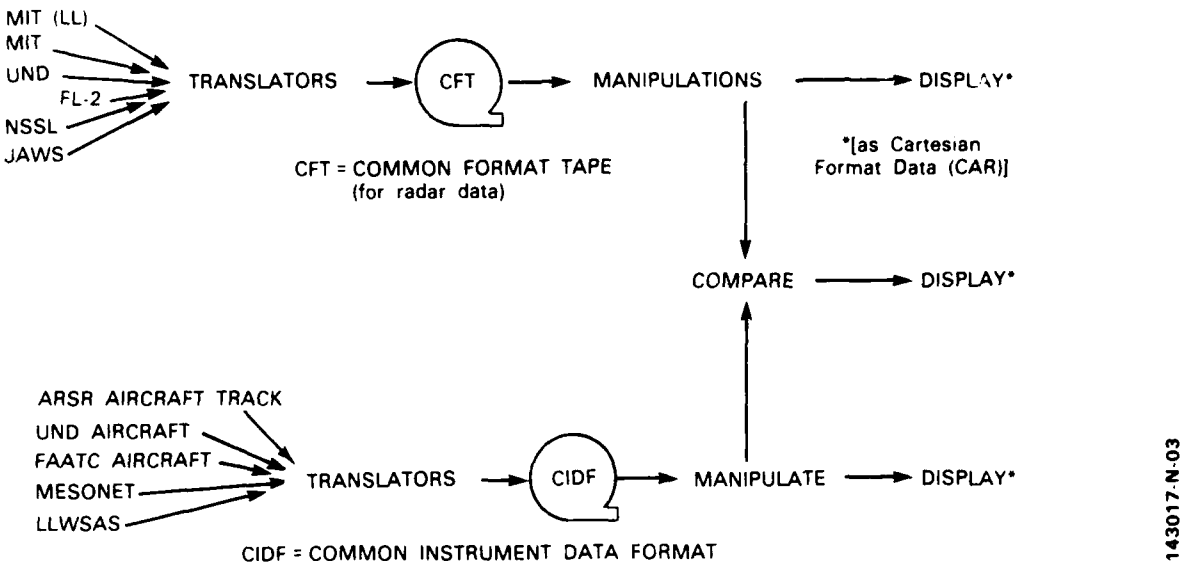

Figure IV-1. Data analysis software structure.

The CAR (cartesian) data format has been restructured to take advantage of product naming, allow more general layer altitude specification, and allow users to read and write real data directly, with built-in scaling features. These changes make the package considerably more potent, while requiring changes in much of our data analysis code.

The RESAMP program, which resamples tilts into cartesian fields, has been updated. It now has the ability to threshold products against a signal-to-noise field. Future enhancements will take advantage of the changes in CAR discussed above.

The FAA requested that we provide examples of NEXRAD layered reflectivity and turbulence maps to MITRE and FAA Technical Center (FAATC) CWP investigators. A translator from CAR to Cartesian Exchange Format (CEF) has been written, and sample tapes sent to the FAATC and the FAA CWP office.

A program is under development that will allow quick display of CAR files. The initial capability will be limited to in-house graphics software displaying plots on a Tektronix 4015, with later versions taking advantage of NCAR graphics software. The program will be capable of displaying contours of radar products, and velocity vector fields.

The NCAR graphics software package has been implemented on the Perkin-Elmer computers. The three routines yet to be adapted satisfactorily had problems with the differences between CDC and Perkin-Elmer hardware and software. The majority of routines have been adapted, and seem to work as advertised. Metacode translators for both the Tektronix 4015 terminal and the Versatec V80 electrostatic plotter have been written, and a spooler for the Versatec to allow multiuser access is being designed.

C. MESONET/LLWAS DATA ANALYSIS

A software package to analyze and process mesonet and LLWAS data has been implemented. This effort involves the use of many different programs as shown in Figure IV-2. A significant amount of processing is devoted to compensating for local (i.e., misoscale) and regional (i.e., mesoscale) reduction of the winds by obstructions. Figure IV-3, taken from Fujita and Wakimoto[1], illustrates the spatial scales of concern. Whereas such blockage effects were not significant in the 'wide open spaces' characteristic of the Denver JAWS experiment, virtually all of the Memphis area mesonet and LLWAS sites have trees relatively nearby in some azimuth sectors. Figure IV-4 shows a panoramic of one site together with the estimated percent of wind blockage as a function of azimuth.

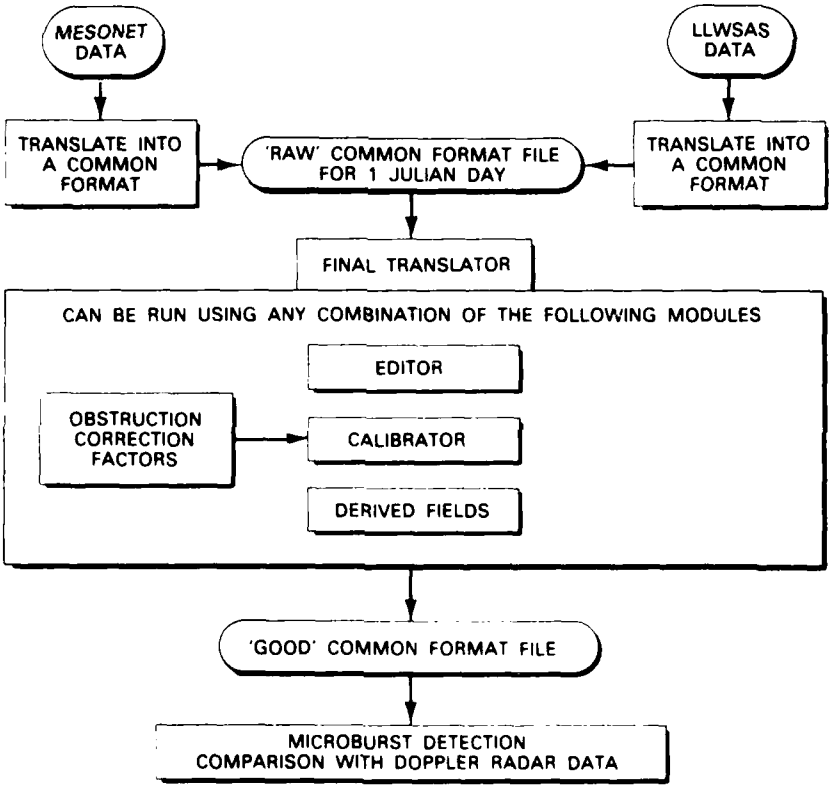

145681 N 01

Figure IV-2. Mesonet/data analysis overview.

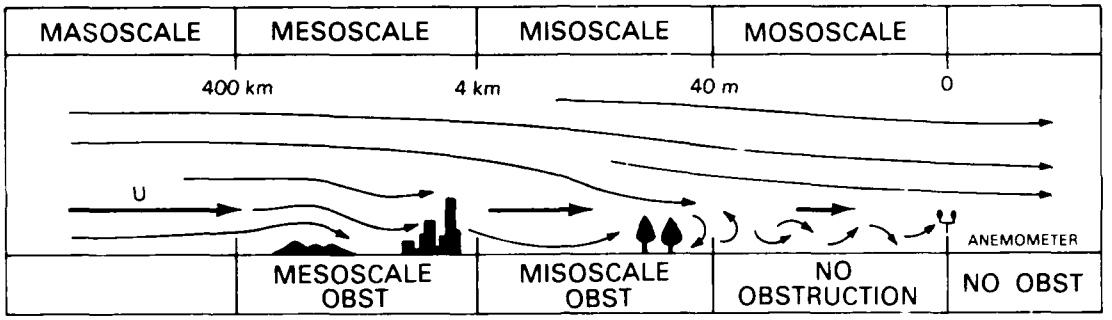

148730-N

Figure IV-3. Obstructions to an anemometer that is located in multiple-scale environment.

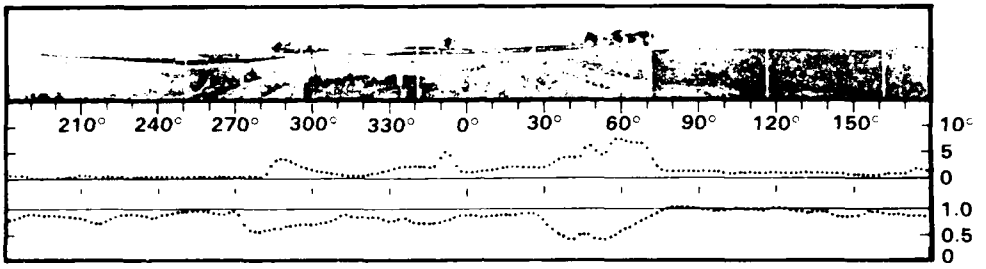

$$\psi = \frac{\text{OBSERVED WIND}}{\text{UNOBSTRUCTED WIND}}$$

148733-R.A

Figure IV-4. Obstruction angles (θ) vs transmission factors (x) at a Memphis mesonet site.

Figure IV-5 shows the obstruction compensation procedure being used. The data from both the Lincoln mesonet (up to 30 stations) and LLWAS System (6 stations, winds only) is translated into our Common Instrument Data Format (CIDF), and all subsequent programs access the data in CIDF. Translation of 1985 LLWAS data (to CIDF) has been completed through February. Because of some slight changes to the Synergetics format and the mesonet translator, the 1985 mesonet data translation has not yet begun.

The capability of calculating a histogram of wind speed versus azimuth for any station for either one day or a series of days (e.g., an entire month) was added this quarter. Also completed was a program that calculates the correlation between transmission factors and smoothed station obstruction angles. This program will allow for the best negatively correlated fit to be used to make azimuthal corrections at each site. Also written was a program that will shift the transmission factors to be aligned with this best negative correlation.

Before any analysis is carried forth, all of the data must be edited. Algorithms have been implemented to reject erroneous values of winds (speed and pressure, relative humidity, precipitation, and temperature). The output of this editor is a list of times at which the

conditions of the algorithm are met. The information is compiled into a data base that then is used as input by another program that deletes the erroneous data.

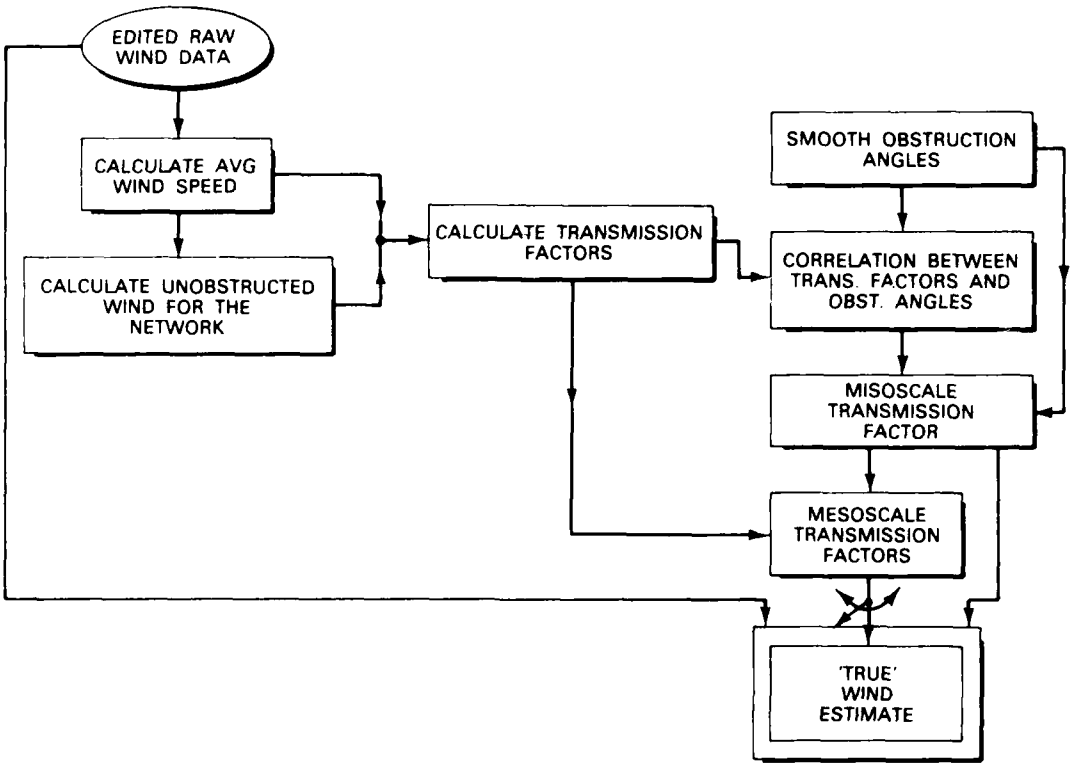

Figure IV-5. Mesonet obstruction compensation.

Editing of all 1984 data was begun this quarter. The final editing translation has been accomplished for the July and October 1984 data. Unobstructed winds and transmission factors were generated from this data and an analysis of the July/October obstruction effects is nearly complete.

The monthly histogram of the July 1984 data set revealed that there was an unacceptable loss of wind direction resolution at 0° and 180° due to the transmission of the cosine only from the wind vane. LLWAS data was used as guidance in correcting this.

Work continued with T. Fujita at the University of Chicago on an improved procedure for correcting winds at sites with visible obstruction greater than about 10°.

Work has begun on a program that will plot the winds (direction and speed) over the entire mesonet. This will help depict how microbursts and/or gust fronts affect surrounding stations at a specified time. The design of a mesonet and LLWAS inventory program has begun. This program will produce a listing of the number of times each sensor at each platform reported missing data and also failed to report.

D. LOW ALTITUDE WIND SHEAR (LAWS) DETECTION ALGORITHM DEVELOPMENT

The low-altitude wind shear (LAWS) detection algorithm development effort is aimed at producing an automatic procedure for recognizing hazardous wind shear events from Doppler weather radar measurements. The current focus of the algorithm development is a simple technique for real-time testing during the 1985 FLOWS experimental program.

The initial version of the algorithm will attempt to identify LAWS hazards (primarily microbursts) by combining several simple feature fields, such as radial shear, azimuthal shear, and local reflectivity maxima. Basic image processing techniques also will be used to spatially smooth and enhance the feature fields.

During this quarter, many of the software utilities needed for the algorithm implementation and analysis were completed. These include programs for:

(1) Computing divergence, convergence, and rotations from the three-dimensional windfields obtained for the NCAR datasets. These fields are used in determining the areas of true hazard.

(2) Computing radial and azimuthal shears from the base radar data (polar format). These shears are fundamental indicators of microbursts and gust fronts. The high resolution shears are computed prior to resampling and layering into a Cartesian coordinate system (CAR format).

(3) Computing local reflectivity maxima cells from layered radar reflectivity fields.

(4) Spatially smoothing any feature field by using a median filter.This program will be used to enhance noisy shear and turbulence feature fields.

(5) Designing weights used for combining separate feature fields into a hazard likelihood map. Figure IV-6 shows the principal features being considered at this time. The weights are determined by minimizing the classification error for a set of test cases.

(6) Comparing a predicted hazard map with a 'truth' field, generated by a human expert. This program computes the overall probability of detection and false alarm for the algorithm. The comparison may be made using either an 'area overlap' or 'flight-path intersection' criteria (Reference 2 describes these criteria).

(7) Plotting vector wind fields (from three-dimensional wind data) superimposed on reflectivity contours. This program is used as an analysis aid in the generation of the truth field.

These programs form the core of the algorithm development and analysis system, and will be used extensively over the next several months. The major software development needed at this point centers on the enhancement of the resampling and layering utility. This program converts a data field sampled in (range, azimuth, elevation) space to one sampled in a uniform cartesian coordinate system, with several altitude layers. The existing version of the utility is quite limited in its capabilities, and will receive considerable attention during the next quarter.

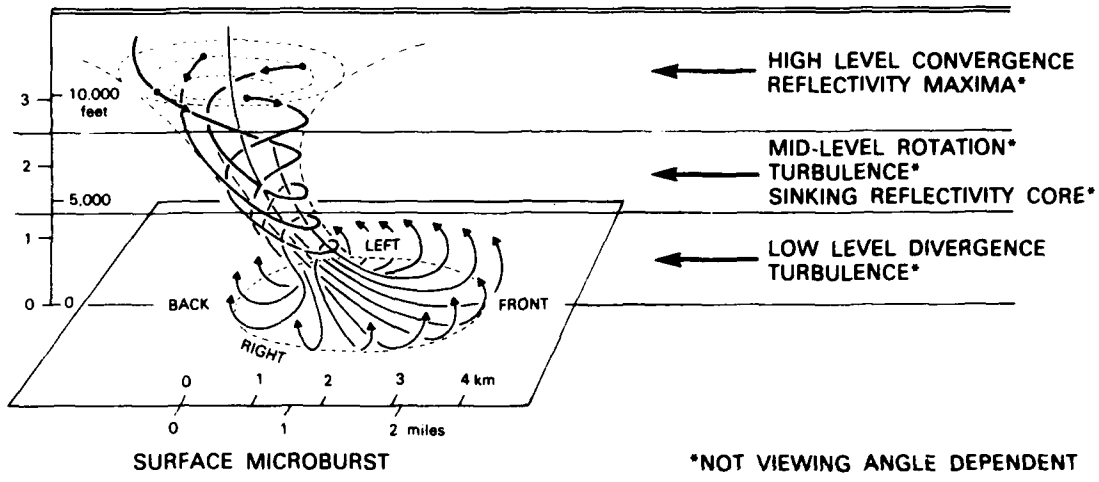

148724-N-01

Figure IV-6. Principal microburst detection features.

All single- and multiple-Doppler radar datasets requested from NCAR have been received, so that we may begin large-scale data analysis. A microburst case being investigated at NSSL also has been identified as useful for our study and will be requested.

The basic altitude limits for the feature layers (low, middle, and high) have been selected, and data processing of a single scan of data from the JAWS project (30 June 1982) has begun. The multiple-Doppler windfields have been used to create a map of areas of actual hazard, and three single-Doppler fields (one from each radar) have been processed. For each radar, the shear fields have been calculated and layered, and reflectivity maxima features have been computed. These products were used in a demonstration of the LAWS algorithm development for an FAA program review held on 5 February.

Many of the microburst cases being used for this study have spectrum width information included in the dataset. This information may be useful as an indicator of *small-scale* shears. The width field for the 30 June case was compared briefly to the other feature fields for that scan, and some correlation between the fields is evident.

The work for the next quarter will focus on processing the datasets currently in hand through the algorithm, and evaluating the results. When the initial algorithm has been characterized and the various parameters have been 'tuned', a real-time implementation will be constructed. In parallel, microburst datasets will be obtained from the FLOWS measurement program for additional algorithm analysis. To allow the construction of three-dimensional windfields from this data, we will implement a multiple-Doppler analysis package. As time permits, the investigation of more sophisticated feature calculation and object detection techniques will be investigated.

E. TURBULENCE ALGORITHM DEVELOPMENT

All of the aircraft data acquired in the 1983 Boston area measurements have been analyzed in greater detail. The turbulent kinetic energy dissipation rate ϵ, a quantity typically used as a turbulence severity indicator was computed using the methods presented by Labitt[3]. These are summarized in Figure IV-7. Meanwhile, the derived gust velocity U_{de}, which was used by Lee[4] to indicate intensity of turbulent air motions in the wind field, was also computed from the equation

$$U_{de} = \frac{2\,\Delta_n\,W_a}{V_e K_g \rho_o C_{L_\alpha} S} \qquad \text{(IV-1)}$$

with

Δ_n = incremental vertical acceleration of aircraft (from normal)

W_a = weight of aircraft

V_e = equivalent airspeed at sea level

ρ_o = air density at sea level

C_{L_α} = aircraft lift curve slope

K_g = gust alleviation factor

S = wing area.

Derived gust velocity has been used by researchers in aircraft dynamics (see, e.g., Reference 5) to translate the normal accelerations encountered by one plane to those for other aircraft. The current data analysis is the first to our knowledge that compares kinetic dissipation rate (used by Labbit[3] and Lewis[6]) and derived gust velocity (used by Lee[4] and Bohne[7,8] from the same aircraft and storms.

To minimize the data bias contributed by a change of aircraft flight altitude, the analysis focuses on data segments where the flight altitude remains constant. Thus, for example, in the case of 15 June 1983 aircraft observational data shown in Figure IV-8, only four legs of data were selected for computing ϵ and U_{de}.

The time series of kinetic energy dissipation rates $\epsilon_p^{1/3}$ calculated from the pressure structure function and $\epsilon_a^{1/3}$ calculated from acceleration sructure are shown in Figures IV-9 and IV-10, respectively. It can be seen from Figures IV-9 and IV-10 that there is a good agreement between $\epsilon_p^{1/3}$ and $\epsilon_a^{1/3}$ resulting from two different methods. The correlation coefficient is 0.74 for the entire flight without removal of bias, and is 0.84 with the removal of bias attributable to change of altitude. Table IV-1 shows the correlation coefficients between $\epsilon_p^{1/3}$ and $\epsilon_a^{1/3}$ for all the flights presented here. In general, for all the cases examined, $\epsilon_p^{1/3}$ is higher than $\epsilon_a^{1/3}$.

ESTIMATION FROM ACCELERATION SPATIAL VARIANCE (D_a):

$$\epsilon^{1/3} = \sqrt{\frac{3D_a}{C}} \quad \frac{m}{C_{L_\alpha} S V^{4/3} T^{1/3} \rho}$$

D_a = $\overline{[a(t+T) - a(t)]^2}$

m = AIRCRAFT MASS

v = TRUE AIRSPEED

ρ = AIR DENSITY

C_{L_α} = AIRCRAFT LIFT CURVE SLOPE

ESTIMATION FROM PITOT TUBE DIFFERENTIAL PRESSURE SPATIAL VARIANCE ($D_{\Delta p}$)

S = WING AREA

$$\epsilon^{1/3} = \frac{\left(\frac{RT_t}{\tau}\right)^{1/3} \left(\frac{\gamma-1}{2\gamma}\right)^{2/3} \sqrt{D_{\Delta P}}}{C^{1/2} \left(1 + \frac{\Delta p}{P_f}\right) \frac{\gamma+2}{3\gamma} \left[\left(1 + \frac{\Delta p}{P_f}\right)^{\frac{\gamma-1}{\gamma}} - 1\right]^{2/3} P_f}$$

$D_{\Delta p}$ = $\overline{[\Delta p(t+T) - \Delta p(t)]^2}$

R = GAS CONSTANT

γ = RATIO OF SPECIFIC HEATS

Δp = PITOT TUBE OF DIFFERENTIAL PRESSURE

p_f = STATIC OR FREE STREAM PRESSURE

p_s = STAGNATION OR TOTAL PRESSURE

T = TIME SPACING BETWEEN MEASUREMENTS

C = 'UNIVERSAL' CONSTANT FOR TURBULENCE

T_t = TOTAL TEMPERATURE

155186-N

Figure IV-7. Techniques for estimating kinetic dissipation rate (ϵ).

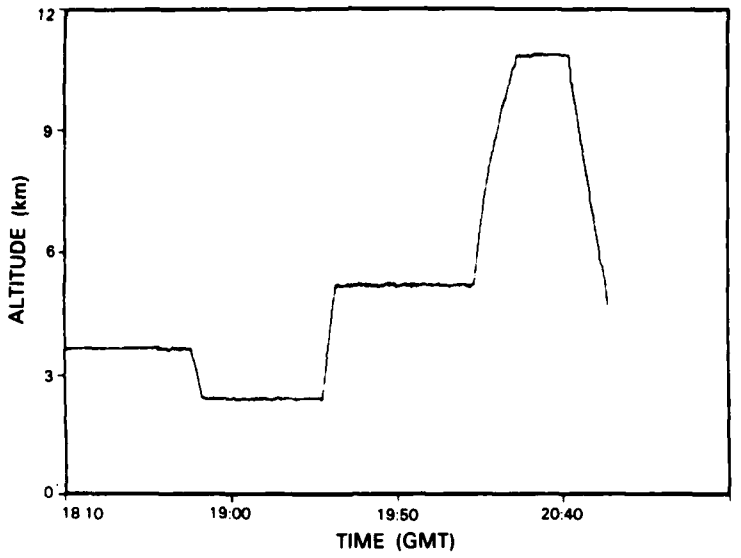

155187-N

Figure IV-8. Aircraft flight altitude profile for 15 June 1983 test.

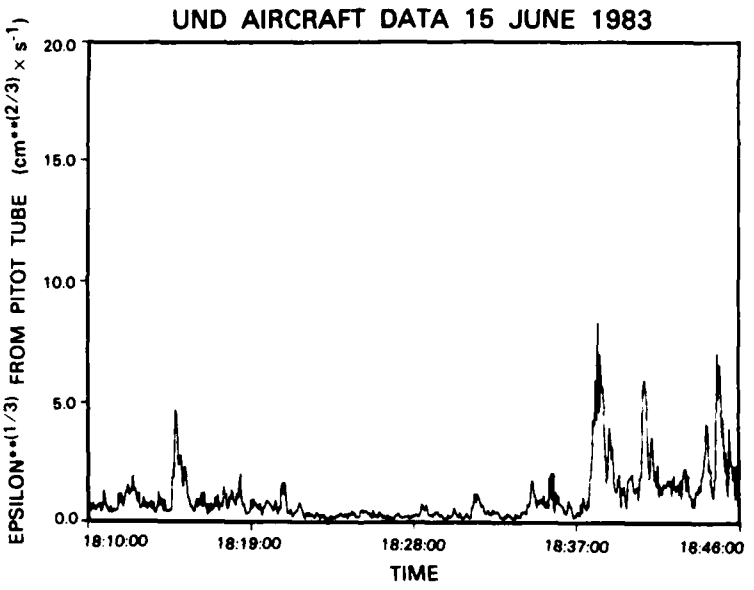

155188-N

Figure IV-9. Kinetic dissipation rate from pressure fluctuation time series for 15 June 1983 flight.

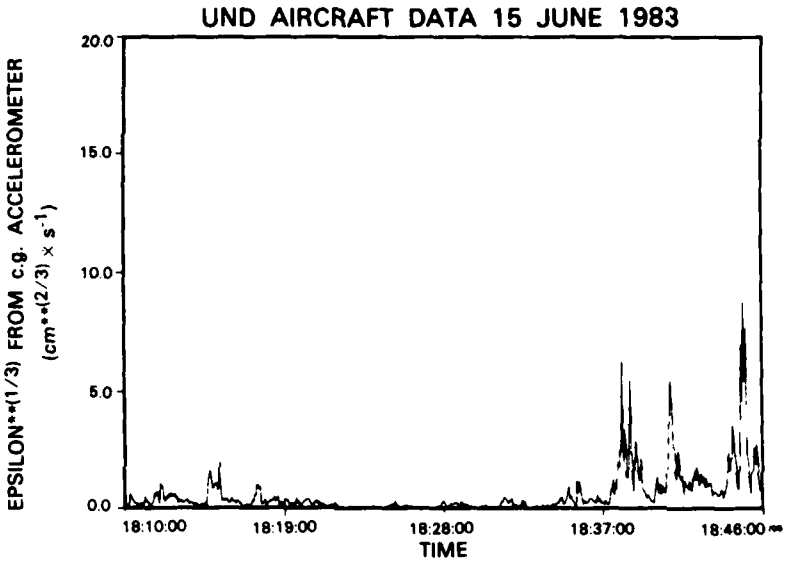

155189-N

Figure IV-10. Kinetic dissipation rate from vertical aceleration time series for 15 June 1983 flight.

TABLE IV-1

Correlation Between $\epsilon_a^{1/3}$ and $\epsilon_p^{1/3}$ Inferred From 15 June 1985 Aircraft Data

Time		Altitude	Correlation Coefficient
Beginning	Ending		
18:10	18:46	~ 3.5 km	0.84
18:50	19:22	~ 2.5 km	0.75
19:27	20:11	~ 5.0 km	0.79
20:22	20:34	~11.0 km	0.59

ϵ_p = dissipation rate computed from pressure structure function

ϵ_a = dissipation rate computed from acceleration structure function

The corresponding time series of U_{de} is plotted in Figure IV-11 for illustration. The distribution of U_{de} is similar to the patterns of $\epsilon_p^{1/3}$ and $\epsilon_a^{1/3}$ shown in Figures IV-9 and IV-10. However, a close examination of the results illustrated in Figures IV-9 through IV-11 reveals that the turbulence intensity scales implied by the various measures are significantly different. For example, over the time interval 18:37 to 18:46, the peak values of $\epsilon_p^{1/3}$ and $\epsilon_a^{1/3}$ indicate a moderate to heavy turbulence, according to the MacCready's[9] scale shown in Figure IV-12. On the other hand, the peak values of U_{de} correspond to a light turbulence level according to the scale in Table IV-2 (from a NACA report[5]).

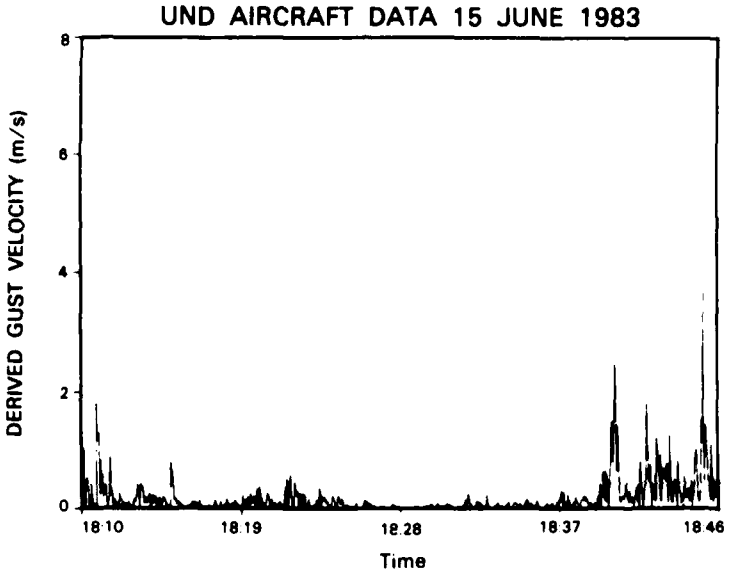

Figure IV-11. Derived gust velocity from vertical acceleration time series for 15 June 1983 flight.

This discrepancy between the various measures of aircraft-encountered turbulence was not observed in the previous Doppler weather radar turbulence detection programs because the investigators considered only kinetic dissipation rate or only derived gust velocity, but not both. This is an important issue to resolve since it impacts significantly on the operational utilization of the turbulence products from NEXRAD and the Terminal Doppler Weather Radar (TDWR). During the next quarter, we will complete a detailed analysis of the other aircraft data from 1983 and consult with aircraft dynamics experts to better understand the practical import of the various turbulence measures.

We commenced a study of the relationship between Doppler spectrum variance σ_u and kinetic energy dissipation rate ϵ to determine the effect of different range normalization schemes, namely, infinite outer scale (Frisch and Clifford[10], Labitt[3]), and finite outer scale (Bohne[7]), on the estimate of ϵ. Our preliminary results clearly indicate that outer scale size is a dominant factor affecting the estimation of ϵ at close ranges. A more comprehensive study of this topic will be undertaken in the next quarter.

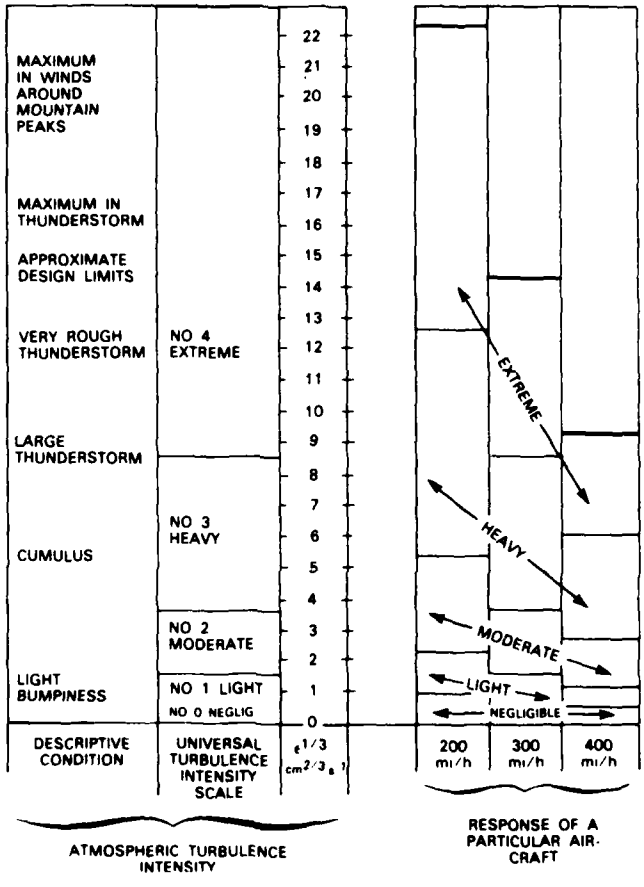

155191-N

Figure IV-12. Turbulence scale suggested by MacCready[9].

TABLE IV-2

Thresholds for Derived Gust Velocity Turbulence Intensity Scale

U_{de}	Turbulence Scale
NASA (Lee)	
$3.0 \leqslant U_{de} \leqslant 6.0$	Light
$6.1 \leqslant U_{de} \leqslant 9.1$	Moderate
$9.2 \leqslant U_{de} \leqslant 12.1$	Severe
$U_{de} \geqslant 12.2$	Extreme
U_{de} = derived gust velocity (m/s)	

Some progress was made in developing software to compare the aircraft-sensed turbulence with the corresponding layered $\epsilon^{1/3}$ or spectrum width fields. We anticipate making quantitative comparisons in the next quarter.

F. CLUTTER ENVIRONMENT ASSESSMENT

Effective radar reflectivity levels of clutter were measured at the Memphis FL-2 site. Further data was recorded after clutter filters were applied. The effective reflectivity levels were computed to determine the clutter suppression by the filters.

Interclutter visibility (ICV) by clutter mapping was simulated using the measured data after it was filtered. The results of the simulation demonstrated that clutter residue can be reduced drastically by clutter mapping even after a clutter filter is used. Figure IV-13 shows the regions where the effective clutter level exceeds the equivalent of +10 dBz at the Memphis site for

(a) the average clutter level in a 0.0625 km^2 cell, and

(b) the lowest clutter level in a 0.0625 km^2 cell.

The average level corresponds to the environment for a system not using a clutter map whereas the minimum level approximates the clutter level in the 'good cells' identified by the clutter map.

Data from Eglin Air Force Base and the Memphis area were reduced to area scattering cross section (σ_o) levels by the Lincoln Air Vehicle Survivability evaluation (AVSE) program staff. These data will be converted from σ_o levels to effective weather reflectivity levels and used to test ICV techniques.

In the next quarter, we will:

(1) Develop software to translate the AVSE program data to CFT format so that ICV can be assessed for these data sets, and

(2) Analytically assess the clutter suppression by clutter mapping by using appropriate probability models for the clutter amplitude distribution.

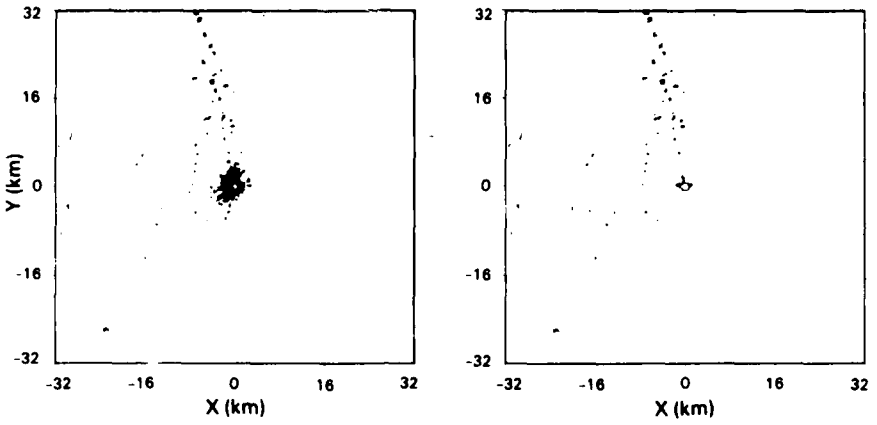

155192-N

THRESHOLDED BLACK AND WHITE MAPS OF RESAMPLED (0.25 km × 0.25 km) CLEAR DAY FILTER OUTPUTS WITH: (a) AVERAGE, (b) MINIMUM VALUE USED FOR RESAMPLING.

Figure IV-13. Effective clutter levels at FLOWS test site.

V. ASSESSMENT OF UTILITY OF NEXRAD PRODUCTS FOR ATC USE

Discussions were held with Lloyd Stevenson of the DoT Transportation Systems Center to obtain data on the impact of weather on Memphis ATC operations as an aid to NEXRAD CWP product optimization. Due to funding constraints, Stevenson will not be able to work in Memphis this coming summer as we had hoped. We are working to develop a very low cost terminal ATC data acquisition program using the college students who will assist in site operations. If suitable students can be hired, we plan to present a data collection plan to Memphis TRACON and tower personnel in late June.

A preliminary design for the graphic displays in the CWP weather radar product demonstration planned for the Memphis ARTCC in September-November 1985 was accomplished. Figure V-1 shows the format for display of the strawman CWP layered products (e.g., precipitation and turbulence regions) along with higher spatial resolution data in order that

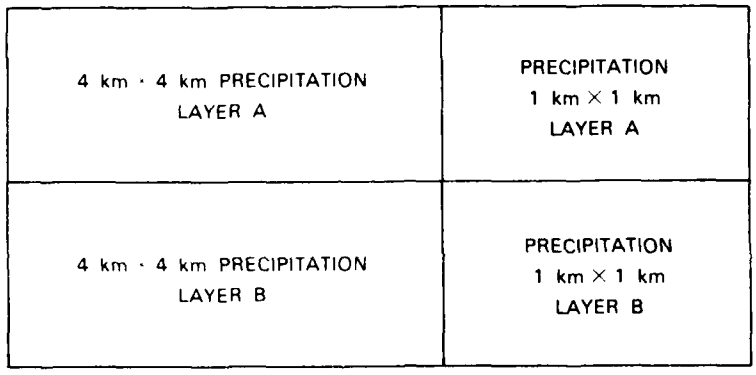

155193-N

Figure V-1. Display of layered reflectivity product.

the CWSU meteorologist can assess the meteorological validity of the layered products. Figure V-2 shows how the Forecast Reflectivity Maps generated by the Correlation Tracker and Storm Extrapolation Map algorithms would be compared with current data and previous predictions. The Apollo workstations to be procured have a quarter screen zoom feature on their 800 × 1000 pixel display so that any particular image can be expanded to fill the screen.

The high resolution of the workstation display also will enable us to display current aircraft locations and ATC beacon data on the color display without unduly obscuring the weather maps. This pseudo Advanced Automatic System (AAS) display mode will permit user feedback on weather product utility in an ATC controller environment.

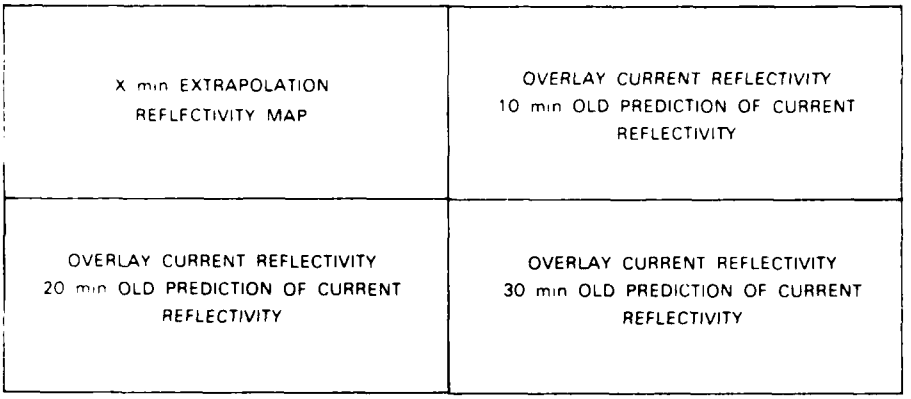

155194-N

Figure V-2. Evaluation of storm extrapolation map product.

VI. SPECIFICATION OF NEXRAD PRODUCTS FOR THE CENTRAL WEATHER PROCESSOR (CWP)

The principal focus of activity in NEXRAD product (N-product) generation studies for the CWP was in the area of correlation tracking and reflectivity extrapolation.

Correlation tracking and reflectivity extrapolation studies carried out during the first quarter of 1985 were directed at evaluations of two correlation-type trackers – the basic correlator documented in Lincoln Project Report ATC-124[2] and a binary correlator developed at Lincoln and at identifying the appropriate N-Product to serve as the input data field to such a tracker.

The binary correlator is structurally similar to the basic correlator; however, it converts the reflectivity fields to be correlated to binary fields through the use of a reflectivity threshold (typically 25 dBZ) prior to the computation of the spatial correlation coefficients. The use of binary data provides for substantial decreases in the algorithm's computational requirements through two mechanisms: the number of multiplications required to compute the correlation coefficient is approximately reduced by a factor of three, relative to the usual computation of that quantity; and many arithmetic operations may be effected through logical comparisons – in general, logical operations are executed more rapidly than arithmetic ones on digital computers. Our evaluations indicate a factor of 4-7 speed advantage for the binary correlator, relative to the basic correlator, for input data fields of the same spatial extent and spatial resolution.

Ken Wilk of the NEXRAD IOTF had noted that the binary correlator tracks the envelope of storm processes and hence might be less susceptible to cell propagation effects in supercell storms than is the basic correlator. To assess the performance, we conducted simulation tests on a subset of the five storm cases considered previously by John Brasunas.[2]

The performance of the two correlation trackers in synoptic conditions characterized by stratiform precipitation with modest convection or extended storms (e.g., squall lines) was comparable for the cases included in the evaluations, and it was recommended to the JSPO that the binary correlator replace the current CROSS-CORRELATION TRACKING [028] algorithm, on the basis of its performance and computational economy.

The data fields evaluated as potential inputs to a correlation-type tracker were high-resolution COMPOSITE REFLECTIVITY (1 km × 1 km × SFC-48 kft (14.7 km)) degraded horizontally to 2 km × 2 km and 3 km × 3 km, low-resolution COMPOSITE REFLECTIVITY (4 km × 4 km × SFC-48 kft), and low-level LAYER COMPOSITE REFLECTIVITY [4 km × 4 km × SFC-18 kft (5.5 km)]. Both trackers appeared to be insensitive to the effects of varying horizontal resolution and vertical extent for the storms considered. The extrapolation time for which extrapolated reflectivity maps (constructed on the basis of the trackers' estimated velocity fields) were most accurate was observed to increase with decreasing resolution (i.e., increasing pixel size). This effect is attributed to the exclusion of small-scale, short-lived reflectivity features, whose motion is not representative of the overall motion of the field, from the trackers' purview by use of the coarser resolutions.

Low-level LAYER COMPOSITE REFLECTIVITY was recommended as the input to a correlation tracking algorithm for the following reasons:

(1) tracker performance using this product as an input was observed to be comparable to that obtained with the COMPOSITE REFLECTIVITY-based inputs,

(2) considerations of computational efficiency dictate the choice of the coarsest acceptable horizontal resolution (computational requirements for the correlation coefficients decrease as the fourth power of the pixel edge length for a fixed spatial area), and

(3) the NEXRAD Technical Requirements guarantee that the LAYER COMPOSITE REFLECTIVITY product will be available to a correlation tracking algorithm in the required cartesian format.

With surrogate LAYER COMPOSITE REFLECTIVITY, out to a 180 km maximum range and excluding Input/Output time, average running times for the binary correlator were on the order of 3 seconds. Our evaluations indicate that this running time is comparable to that required by the tracking logic of the centroid tracker — the current Category I NEXRAD reflectivity tracker.

Lincoln personnel attended several meetings on RRWDS data processing in the CWP. We recommended:

(1) a clear day clutter map be used to suppress clutter in the RRWDS data rather than relying only on adjacent RRWDS sensor coverage since the adjacent sensors may not have line-of-sight (LOS) visibility of low altitude precipitation,

(2) a simplified functionally stated resampling approach [such as has been incorporated in the NEXRAD Technical Requirement (NTR) for layered product generation] be used for the CWP RRWDS processing, and

(3) that steps be taken to record appropriate storm and clutter data at the FAATC this spring and summer for RRWDS processing validation.

Work commenced on an algorithm to generate the arbitrary vertical cross section product described in the September 1984 Quarterly Technical Summary. The initial focus is an algorithm that utilizes resampled tilt data (i.e., data on a Cartesian grid) since this format will be produced real-time at the FL-2 radar site and is available offline at Lincoln. After an initial capability is generated and evaluated, a refined version will be specified next quarter.

REFERENCES

1. T. Fujita and R. Wakimoto, "The Effects of Miso- and Mesoscale Obstructions on PAM Winds Obtained During Project NIMROD," J. of Appl. Meteorol. **21**, 840-858 (1982).

2. J. Brasunas, "A Comparison of Storm Tracking and Extrapolation Algorithms," Project Report ATC-124, Lincoln Laboratory, MIT (31 July 1984), DTIC AD-A146638/2.

3. M. Labitt, "Coordinated Radar and Aircraft Observations of Turbulence," Project Report ATC-108, Lincoln Laboratory, MIT (6 May 1981), DTIC AD-A114708/1.

4. J.T. Lee, "Application of Doppler Weather Radar to Turbulence Measurements Which Affect Aircraft," Final Report FAA-RD-77-145 to Systems Research and Development Service, FAA, Washington, D.C. (1977).

5. K.G. Pratt and W.G. Walker, "A Revised Gust-Load Formula and Reevaluation of V-G Data Taken on Civil Transport Airplanes from 1933 to 1950," National Advisory Committee for Aeronautics, Report 1206 (1954), pp. 1-4.

6. W. Lewis, R.G. Oliver, A. DelaMarche, and T.Y. Lee "Test and Evaluation of the Radar Thunderstorm Turbulence Detection System (Phase I)," FAA Technical Center Report DOT/FAA/RD-82/22 (July 1982).

7. A.R. Bohne, "Radar Detection of Turbulence in Precipitation Environments," J. Atmos. Sci. **39**, 1819-1837 (1982).

8. A.R. Bohne, "Radar Detection of Turbulence in Thunderstorms," Air Force Geophysics Laboratory Report, AFGL-TR-81-0102 (March 1981).

9. P. MacCready, "Standardization of Gustiness from Aircraft," J. of Appl. Meteorol. **3**, 439-449 (1964).

10. A.S. Frisch and S.F. Clifford, "A Study of Convection Capped by a Stable Layer Using Doppler Radar and Acoustic Echo Sounders," J. Atmos. Sci. **31**, 1622-1628 (1974).

PRINCIPAL CONTRIBUTORS

The principal contributors to this report were M.M. Wolfson, J.T. DiStefano, M.H. Goldburg, M.W. Merritt, Y. Lee, B.A. Rapaport and D.R. Mann.

GLOSSARY

AAS	Advanced Automatic System
A/D	Analog-to-Digital
AGC	Automated Gain Control
ARTCC	Air Route Traffic Control Center
ATC	Air Traffic Control
AVSE	Air Vehicle Survivability Evaluation
CAR	Cartesian
CDC	Control Data Corporation
CEF	Cartesian Exchange Format
CFT	Common Format Tape
CIDF	Common Instrument Data Format
CWP	Central Weather Processor
CWSU	Center Weather Service Unit
DAA	Data Acquisition and Analysis (Processor)
dBZ	Weather Reflectivity
DCP	Data Collection Platform (implies transmitter to GOES satellite)
FAA	Federal Aviation Administration
FAATC	Federal Aviation Administration Technical Center
FLOWS	FAA/Lincoln Operational Weather Studies
FL-2	FAA/Lincoln Laboratory Test-Bed Doppler Radar
GOES	Geostationary Operational Experimental Satellite
HDLC	High Level Data Communications
ICV	Interclutter Visibility
IOTF	Interim Operational Test Facility
JAWS	Joint Airport Weather Studies
JDOP	Joint Doppler Operational Program
JSPO	Joint System Program Office (for NEXRAD program)
LAWS	Low-Altitude Wind Shear
LOS	Line-of-Sight
LLWSAS	Low-Level Wind-Shear Alert System
MB	Megabyte
mesonet	Refers to a network of automatic weather stations with a close spacing, i.e., a 'mesoscale' spacing. Lincoln's spacing might be called 'microscale.'
MTS	Moving Target Simulator

NCAR	National Center for Atmospheric Research, Boulder, Colorado
NEXRAD	Next Generation Weather Radar
NSSL	National Severe Storms Laboratory, Norman, Oklahoma
NTR	NEXRAD Technical Requirement
OS 32	Perkin-Elmer Operating System
P.E.	Perkin-Elmer
RHI	Radial Height Indicator
RRWDS	Radar Remote Weather Display System
SGP	Single Gate Processor
SP	Signal Processor
TDWR	Terminal Doppler Weather Radar
UND	University of North Dakota
UNIX	'Generic' operating system developed by Bell Laboratories

END

FILMED

1-86

DTIC